

## An innovative design of a frequency-tunable UHF RFID antenna for identification applications

Zakaria Errachidi<sup>1</sup>, Jamal Zbitou<sup>1,2</sup>, Noha Chahboun<sup>1</sup>, Otman Oulhaj<sup>3</sup>, Ahmed Lakhssassi<sup>4</sup>

<sup>1</sup>Information and Communication Technologies Laboratory, National School of Applied Sciences of Tangier, Abdelmalek Essaadi University, Tetouan, Morocco

<sup>2</sup>ENSA of Tetouan, Abdelmalek Essaadi University, Tetouan, Morocco

<sup>3</sup>TEDAEPP Research Team, Faculty Polydisciplinary Larache, Abdelmalek Essaâdi University, Tetouan, Morocco

<sup>4</sup>Department of Engineering and Computer Science, University of Quebec in Outaouais, Gatineau, Canada

### Article Info

#### Article history:

Received Nov 9, 2024

Revised Jul 10, 2025

Accepted Jul 29, 2025

#### Keywords:

Alien H4 RFID micro-chip  
Frequency-tunable  
Impedance matching  
Radio frequency identification  
Rogers 4350B  
Split-ring resonators  
Ultra-high frequency

### ABSTRACT

This paper introduces the design of a new frequency-reconfigurable ultra-high frequency radio frequency identification (UHF RFID) antenna, demonstrating an innovative approach that enables dynamic adjustment of its resonance frequency. The proposed antenna design features a central dipole structure, enhanced by two hexagonal split-ring resonators (H-SRR) at each end. A T-match network is integrated into the center of the dipole, which is essential for achieving impedance matching between the antenna and the Alien Gen2 H4 RFID microchip. The antenna is designed using a Rogers 4350B substrate, a high-performance dielectric material ideal for RFID applications. With dimensions of  $68 \times 32.6 \times 1.524$  mm<sup>3</sup>, the compact antenna maintains full UHF band (860 MHz to 930 MHz) coverage compliant with International Telecommunications Union (ITU) RFID standards. This ensures that the antenna can be used in different regions around the world, offering broad compatibility with various RFID systems. The antenna's frequency reconfigurability is achieved through the integration of localized capacitors with variable values, which plays a key role in enabling precise adjustments to the antenna's center frequency across the entire UHF band. Extensive simulation results validate the effectiveness of this reconfigurable design, demonstrating that the antenna can dynamically adjust its frequency while maintaining excellent performance metrics, including impedance matching, radiation efficiency, and bandwidth. This makes the proposed antenna an ideal choice for modern RFID applications.

This is an open access article under the [CC BY-SA](https://creativecommons.org/licenses/by-sa/4.0/) license.



### Corresponding Author:

Zakaria Errachidi  
Information and Communication Technologies Laboratory  
National School of Applied Sciences of Tangier, Abdelmalek Essaadi University  
Tetouan, Morocco  
Email : zakaria.errachidi@etu.uae.ac.ma

## 1. INTRODUCTION

Reconfigurable antennas are advanced devices capable of dynamically altering their electromagnetic properties in response to specific needs. Unlike traditional antennas with fixed characteristics, these antennas can adjust their frequency, polarization, directivity, radiation pattern, or impedance in real time [1]-[4]. This reconfigurability is made possible through the integration of active or passive components within the antenna structure, such as varactor diodes [5], [6], PIN diodes [7], [8], microelectromechanical systems (MEMS) [9], or smart materials [10], [11]. This adaptability makes reconfigurable antennas particularly valuable in fields such as wireless communications, radio frequency identification (RFID) tags, radar systems, satellites, and

5G networks [12], where efficiency, flexibility, and interference reduction are crucial. These antennas provide an innovative solution to the increasingly complex challenges of spectrum management and optimization in modern communication systems. Regulating different frequency bands is essential to ensure effective and interference-free use of electromagnetic spectra, which are limited and valuable resources. Each country or region establishes specific rules and standards for allocating frequency bands to various applications such as broadcasting, mobile communications, navigation services, and data networks. For instance, frequency bands for wireless communications are typically regulated to prevent interference between different systems; each band is often subdivided into multiple channels to allow simultaneous use by several operators in accordance with the electronic product code (EPC) Gen2 standard, ultra-high frequency radio frequency identification (UHF RFID) systems use frequency bands between 860 and 930 MHz. In Europe, the frequency range is 865-868 MHz, while in the USA, its range is 902-930 MHz. Table 1 provides a summary of the UHF frequencies that can be used for RFID systems [13].

Table 1. Worldwide distribution of UHF frequencies for RFID applications compliant with the EPC Gen2 standard

860 MHz	Europe 865-868 MHz					India 865-867 MHz			
	USA	Brazil	Arg	Korea	Japan	Aus	Taiwan	China	Thailand
930 MHz	902-928	902-928	902-928	917-921	916-921	920-926	922-928	920-925	920-925

## 2. THE COMPREHENSIVE THEORETICAL BASIS

### 2.1. Hexagonal split-ring resonator

Split ring resonators (SRRs) are ring-shaped resonant metal structures commonly used in metamaterials and antenna design to manipulate the electromagnetic properties of devices, such as achieving negative effective permeability [14], [15]. An SRR consists of two concentric rings with one or more gaps that disrupt the surrounding electromagnetic field, creating resonance at specific frequencies. This compact design can generate a strong magnetic response in devices that would otherwise be too small to interact effectively with the magnetic fields of electromagnetic waves. Due to their ability to adjust the permeability and permittivity of a material, SRRs are widely used in the design of reconfigurable antennas, microwave filters [16], [17], and negative refractive index metamaterials, enabling new applications in the communication, detection, and control of electromagnetic waves.

This study explores a novel RFID passive tag structure designed for the UHF band, based on a hexagonal split-ring resonator (H-SRR) configuration [18]. Figure 1 illustrates a schematic of the H-SRR, which consists of two concentric metal rings with different diameters and dimensions, each featuring a split gap on opposite sides. In this design,  $g_1$  and  $g_2$  represent the split gaps in the inner and outer rings, respectively;  $w$  denotes the width of the metallic strips, and  $d$  is the distance between the rings.

The H-SRR can be modeled using an equivalent electrical circuit that functions as a resonant cavity [18], similar to an LC circuit with a resonance frequency  $f_0$ . In this model, the rings provide the inductive component ( $L$ ) of the SRR, whereas the capacitive component ( $C$ ) is due to the spacing between the rings and the gaps within each ring. Figure 2 shows the electrical circuit corresponding to the H-SRR configuration.

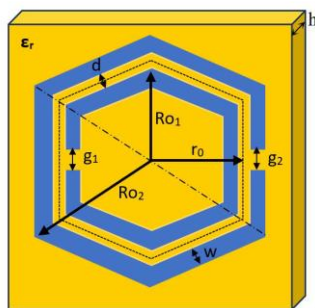


Figure 1. Geometry of the H-SRR

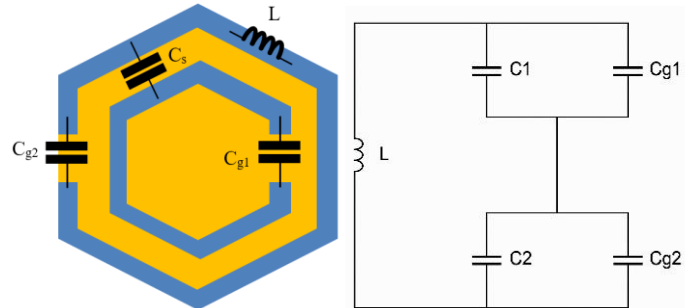


Figure 2. Electrical schematic for H-SRR

The resonance frequency  $f_0$  of the H-SRR is given by (1), as mentioned in [18].

$$f_0 = \frac{1}{2\pi\sqrt{L_T C_{eq}}} = \frac{1}{2\pi\sqrt{L_T \left[ \frac{(3r_0 - g_1)C_{pul}}{2} + \frac{\epsilon_0 ch}{2g_1} \right]}} \quad (1)$$

where  $L_T$ , the total inductance of the structure, is determined by (2):

$$L_T = 0.005081 \left( 2.303 \log_{10} \frac{4l}{w} - \theta \right) \quad (2)$$

$\theta$  is a constant that depends on the geometry of the resonator shape. For a hexagonal resonator, it is defined as follows:  $\theta = 2.636$ , while  $l$  and  $W$  denote the wire length, and width respectively.

The equivalent capacitance  $C_{eq}$  of the structure is determined using the equivalent circuit shown in Figure 3 and the formula provided in (1). In this context,  $C_{pul}$  denotes the capacitance per unit length between the rings, while  $r_0$  represents the average radius of the SRR in question. The value of  $C_{pul}$  is calculated as detailed in references [18], [19].

$$C_{pul} = \frac{\sqrt{\epsilon_e}}{c_0 Z_0} \quad (3)$$

Here,  $\epsilon_e$  represents the medium's effective permittivity,  $Z_0$  is the medium's impedance, and  $c_0 = 3 \times 10^8$  m/s denotes the speed of light in a vacuum.

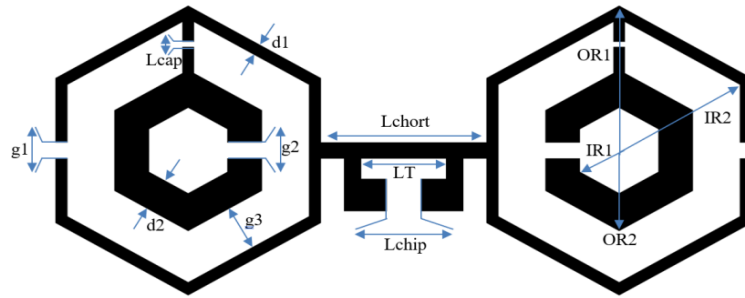


Figure 3. Electrical schematic for H-SRR

Reconfiguring SRRs with capacitors of different values represents an innovative approach to energize and adapt these resonators [20]-[22]. This method involves integrating or adjusting variable capacitors within the SRR structure, allowing for flexible and controllable modifications of its electromagnetic properties. By varying these capacitor values, it is possible to alter the resonator's resonance frequency, modulate its impedance, and meet specific requirements without the need for a complete redesign of the device. The integration of variable capacitors can be achieved in several ways [23], [24]. For example, varicap diodes, which allow modulation of capacitance based on the applied voltage, can be incorporated into the SRR circuit. Similarly, the use of MEMS components with adjustable capacitance or variable capacitive structures mounted on movable elements can also dynamically alter the SRR's characteristics. This approach enables the creation of a resonator whose resonance frequency can be adjusted in real time, providing significant flexibility for applications such as adaptive filters, reconfigurable antennas, and smart communication devices. Integrating an active element into a structure, such as MEMS devices, varicap diodes, or other components requiring external power [25], presents a significant challenge, especially for applications like passive RFID tags. Passive RFID tags, by their nature, do not have their own integrated power source and rely entirely on the energy provided by the RFID reader through radio waves. To overcome these limitations, we replaced the active elements with passive localised capacitors of different values.

### 3. METHOD

#### 3.1. The basic structure of the H-SRR UHF RFID tag

The basic structure of the H-SRR RFID tag studied behaves like a dipole with two ring resonators fused on either side. This configuration can provide the inductive input impedance required to match the conjugate impedance of the chip, and to improve the flexibility of impedance matching, a T-match network is integrated into the centre of the antenna. The tag was modelled on a Rogers 4350B substrate [26], with a thickness of 1.524 mm, a permittivity of 3.66 and a loss tangent of 0.0037. Figure 3 shows the geometry of

the base structure of the proposed tag, while Table 2 presents its optimized parameters. To assess the influence of metal on RFID antennas, this structure is placed on a 20 cm<sup>2</sup> metal plate throughout the simulation phase. It should be noted that the plate's thickness does not affect the label parameters [27].

Table 2. Optimized parameters of the basic structure

Parameter	Dimension (mm)	Parameter	Dimension (mm)
OR1	13.5	Wchort	1.5
OR2	7.5	Lchort	14.563
IR1	12.3	LT	7.5
IR2	4	Lchip	3
g1	1.5	Lcap	0.5
g2	1.5	d1	1
g3	4.157	d2	3.5

### 3.2. Radio frequency identification micro-chip

The Alien Gen2 Higgs-4 micro-chip, mounted on standard strap packaging and integrated in the RFID tag, offers optimal performance for and writing data. According to its data sheet, this chip has a parallel resistance of  $R_p=1.8$  k $\Omega$  and a parallel capacitance of  $C_p=0.89$  pF, offering high reading sensitivity of -20.5 dBm, which enhances to its stability and efficiency in communication. Higgs-4's RFID technology enables fast and reliable identification, even in complex environments, due to its capacity to operate at high frequencies and resist interference. The location of the chip on the RFID antenna is shown in Figure 4 [28].

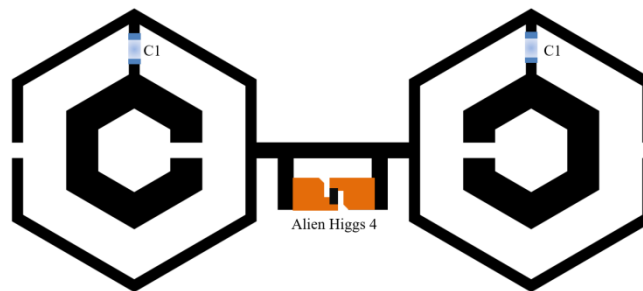


Figure 4. Location of RFID chip on the antenna

The internal impedance of an RFID chip is a crucial factor that affects the quality of communication between the chip and the antenna. Optimal impedance matching between the chip and the antenna directly influences the efficiency with which the tag can absorb and reflect RF signals, this impedance can be calculated at different frequencies using (5), based on the parameters of the parallel resistance  $R_p$  and the parallel capacitance  $C_p$  provided in the Alien H4 chip's datasheet [28].

$$Z_{chip} = R_s - j X_s \quad (4)$$

$$Z_{chip} = \frac{R_p}{1 + (\omega C_p R_p)^2} - j \frac{\omega C_p R_p^2}{1 + (\omega C_p R_p)^2} \quad (5)$$

$$C_s = \frac{1}{X_s \times \omega} \quad (6)$$

Throughout the simulation process, it is crucial to configure a series resistor-capacitor (RC) dipole using the model parameters resistance serie ( $R_s$ ) and condensateur serie ( $C_s$ ) to substitute the chip's input impedance. Table 3 presents the values of these parameters for the standard center frequencies of UHF RFID applications, along with the chip's input impedance at each frequency.

Table 3. Parameters of the Alien H4 chip at UHF RFID frequencies

Central frequency (MHz)	Chip impedance	$R_s$ ( $\Omega$ )	$C_s$ (pF)
865	$Z_{chip}=23.43-j204.043 \Omega$	$R_s=23.43$	$C_s=0.9017$
868	$Z_{chip}=23.27-j203.356 \Omega$	$R_s=23.27$	$C_s=0.9016$
915	$Z_{chip}=20.97-j193.160 \Omega$	$R_s=20.97$	$C_s=0.9004$
920	$Z_{chip}=20.75-j192.135 \Omega$	$R_s=20.74$	$C_s=0.9003$
930	$Z_{chip}=20.30-j190.116 \Omega$	$R_s=20.30$	$C_s=0.9001$

## 4. RESULTS AND DISCUSSION

### 4.1. Frequency reconfigurable H-SRR UHF RFID tag

The integration of a localized capacitance into the spacing between the two rings of the H-SRR structure of the RFID tag, as shown in Figure 5, has enabled control over the antenna's resonance frequency. This method allows for adjusting the central frequency of the antenna according to specific needs, thus providing increased flexibility to adapt to different usage zones. The results obtained with this approach are presented below, highlighting the significant impact of this technique on the performance of our structure.

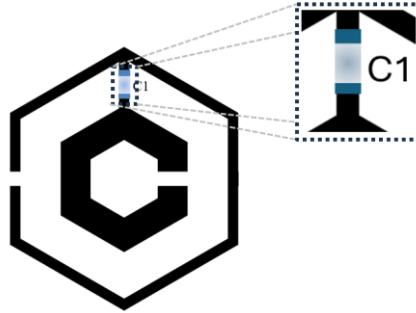


Figure 5. The localized capacitance integrated into the tag

Vishay high frequency (VJ HIFREQ) capacitors are specially designed for high frequency (HF), UHF and microwave (MW) applications, offering outstanding performance in a wide range of electronic and microwave circuits. According to their data sheet [29], capacitance values can vary from 0.1 pF to 91 pF for the reference we have chosen, in this study, the capacitance will be maintained between 0.05 and 0.77 pF. This variation causes the resonant frequency to shift from 930 to 865 MHz, due to the evolution of the  $TM_{10}$  fundamental mode.

### 4.2. Reflection coefficient S11 and impedance matching

According to Figure 6, the variation in the capacitance of the localized capacitor results in an inverse shift in the central frequency; as the capacitance value increases, the central frequency to move to lower values. Table 4 summarizes of the results obtained from this simulation. Notably, all the simulated values of the reflection coefficient are substantial, regardless of the resonance frequency, ensuring adequate impedance matching for the proper functioning of the tag. In fact, a better match between the two impedances leads to a lower reflection coefficient, allowing the chip to receive the maximum transmitted power.

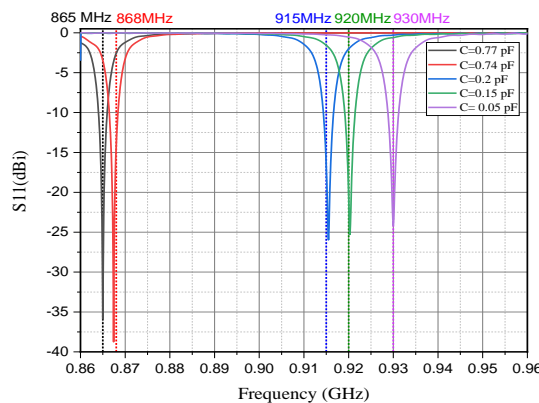


Figure 6. Simulated reflection coefficient S11 for different capacitance values

The illustrations in Figures 7(a)-(e) confirm that the impedance of the simulated antenna is well matched with that of the RFID chip across all frequencies. The real and imaginary values of the antenna's impedance closely approach those of the conjugate impedance of the chip,  $Z_{ant} \approx Z_{chip}^*$ . The simulated impedance values are compared with those of the chip for each frequency in Table 5.

Table 4. The maximum value of the S11 coefficients as a function of the variation in capacitor capacitance for each UHF frequency

Frequency (MHz)	Capacitance (pF)	Simulated reflection coefficient S11 (dBi)
865	0.77	-35.86
868	0.74	-29.52
915	0.20	-16.96
920	0.15	-20.20
930	0.05	-24.16

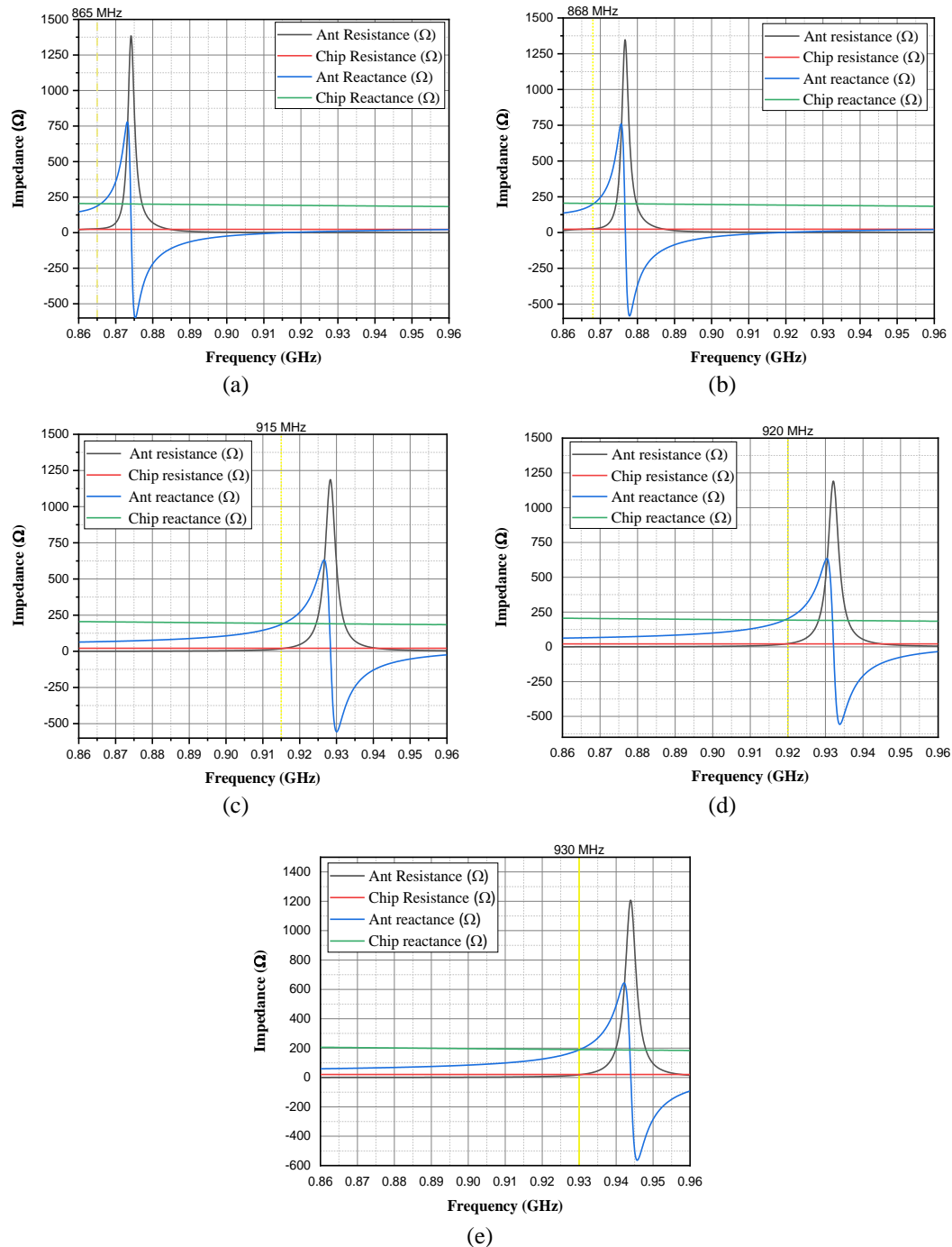


Figure 7. Simulated input impedance of reconfigurable H-SRR RFID antenna with optimised parameters for different values of inserted capacitance; (a) C=0.77 pF, (b) C=0.74 pF, (c) C=0.20 pF, (d) C=0.14 pF, and (e) C=0.15 pF

Table 5. Comparison of impedances: antenna vs chip as a function of the central frequency

Frequency (MHz)	Antenna impedance	RFID chip impedance
865	$Z_{Ant}=27.62+j187.81 \Omega$	$Z_{chip}=23.43-j204.043 \Omega$
868	$Z_{Ant}=26.64+j202.05 \Omega$	$Z_{chip}=23.27-j203.356 \Omega$
915	$Z_{Ant}=18.22+j185.75 \Omega$	$Z_{chip}=20.97-j193.160 \Omega$
920	$Z_{Ant}=22.92+j203.04 \Omega$	$Z_{chip}=20.75-j192.135 \Omega$
930	$Z_{Ant}=18.54+j188.26 \Omega$	$Z_{chip}=20.30-j190.116 \Omega$

#### 4.3. Gain, reading range, and 3D radiation pattern simulation

Having good impedance matching is essential for the effective design of an RFID antenna; however, it is not the only factor to consider. Other key factors, such as gain and the maximum reading distance between the tag and the RFID reader [30] also play an important role in the operation of the RFID system, particularly in far-field applications. The maximum reading distance can be determined using Friis's (7):

$$Rr = \frac{c}{4\pi f_0} \sqrt{\frac{EIRP \cdot G_{ant} \cdot \tau}{P_{th}}} \quad (7)$$

where:  $C$  represents the speed of light in a vacuum, which is equal to  $3 \times 10^8$  m/s,  $f_0$  denotes the center frequency,  $P_{th}$  refers to the minimum RF communication power required to activate the chip (known as the chip's sensitivity), which is -20.5 dBm for the Alien H4 strap microchip, effective isotropic radiated power (EIRP): stands for (EIRP), set at 3.3 W in the European band ([865-868] MHz) and 4 W in the North American band ([902-930] MHz), and  $\tau$  is the power transmission coefficient, calculated using (8), which accounts for the impedance mismatch that may occur between the chip and the antenna.

$$\tau = 1 - \left| \frac{Z_{chip} - Z_{ant}^*}{Z_{chip} + Z_{ant}} \right|^2 = \frac{4R_{chip}R_{ant}}{(R_{chip} + R_{ant})^2 + (X_{ant} - X_{chip})^2} \quad (8)$$

The transmission coefficient quantifies the fraction of power of a signal that is actually transmitted from the RFID reader to the antenna, relative to the initial power of the signal. At the resonance frequency, the transmission coefficient often reaches maximum values, indicating optimal energy transmission by minimizing losses and enhancing signal quality.

The gain of an RFID antenna is a fundamental parameter that measures how efficiently the antenna converts electrical energy into radio waves and vice versa. It indicates the antenna's ability to direct energy in a specific direction, enhancing the range of wireless communication. Figure 8 illustrates the simulated gain curve of the reconfigurable H-SRR antenna as a function of frequency. The curve indicates that the peak gain, when the antenna is positioned directly on a metal plate, at the resonance frequency of 865 MHz with a gain of -5.5 dBi; at 868 MHz, it is -5.48 dBi; at 915 MHz, it is -4.8 dBi; at 920 MHz, it is -4.7 dBi; and at 930 MHz, it is -4.69 dBi. However, this value becomes positive when the antenna is either completely or partially detached from the metal plate.

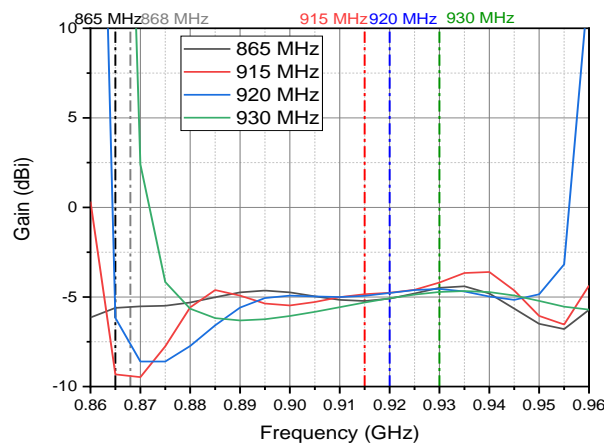


Figure 8. The simulated gain as a function of frequency



It is important to note that each simulated frequency value corresponds to a capacitance value integrated into the antenna. Figures 9(a)-(e) displays the radiation pattern associated with each frequency value, illustrating that the antenna exhibits a directional radiation pattern along the (OZ) axis for the various resonance frequencies.

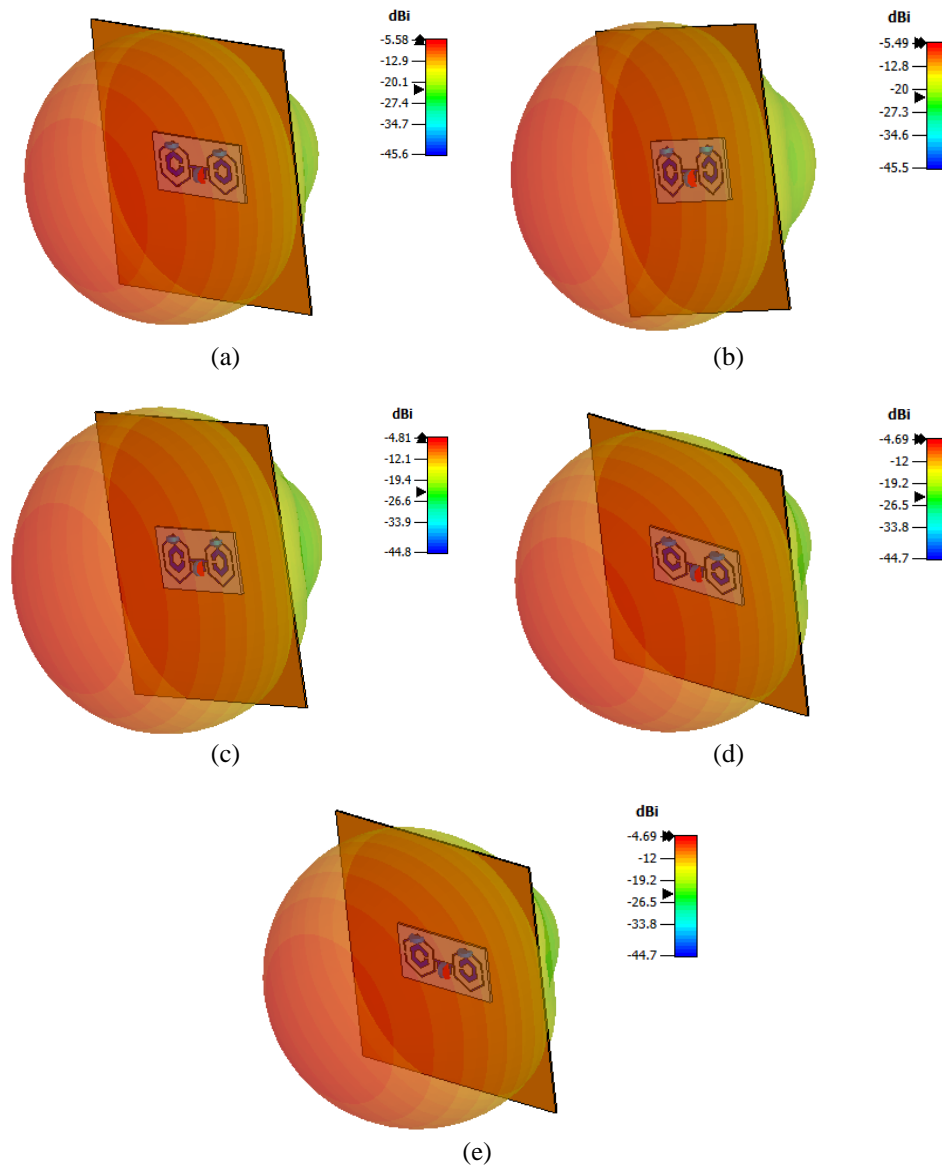


Figure 9. Simulated 3D radiation pattern; (a) 865 MHz, (b) 868 MHz, (c) 915 MHz, (d) 920 MHz, and (e) 930 MHz

By considering the simulated gain values of this antenna, its previously calculated transmission coefficient, and applying Friis's in (7), we obtain calculated read range values based on the applied resonance frequency, as detailed in Table 6.

Table 6. The calculated read range of the reconfigurable antenna

Frequency (MHz)	Gain	EIRP	Transmission coefficient at the resonance frequency	Reading range (m)
865	-5.57	3.3	0.902	8.39
868	-5.48	3.3	0.986	8.87
915	-4.81	4	0.96	9.84
920	-4.75	4	0.938	9.75
930	-4.69	4	0.995	10



Table 7 provides a detailed comparison between the reconfigurable H-SRR antenna developed in this study and existing reconfigurable or dual-band designs. This analysis highlights key RFID tag characteristics including gain, read range, and metal surface compatibility.

Table 7. Performance comparison table of the proposed H-SRR reconfigurable antenna with other reconfigurable and dual-band architectures from the literature

Ref	Metal-mountable	Reconfiguration	Tag volume (mm <sup>3</sup> )	Reconfiguration technology	Need for an external power supply	Gain in free space	Gain on metallic plate	Reading range
[31]	No	Yes	90×25×1.6	diode pin	Yes	1.7 dB at 868 MHz 1.8 dB at 928 MHz	-----	Free space 17.7 m at 868 MHz 20.03 m at 928 MHz
[32]	No	No	73×53×0.8	dual-band	No	2.19 dBi	-----	Free space 9.2 m at 866 MHz, 9.5 m at 915 MHz
[33]	Yes	No	39×39×1.38	dual-band	No	-----	-5.69 dBi at 868 MHz -5.18 dBi at 921 MHz	8 m at 866 MHz, 9 m at 915 MHz
Presented antenna	Yes	Yes	68×32.6×1.524	localized capacitors	No	1.636 dBi at 868 MHz [14]	-4.69 dBi at 930 MHz, -5.57 dBi at 865 MHz	Free space 19.14m at 868 MHz/on metallic plate 8.39m at 865 MHz, 10m at 930 MHz

The proposed tag stands out due to its miniaturized size. Like most metal-mount antennas, it exhibits negative gain that becomes positive when attached to non-metallic materials. Moreover, it achieves an exceptionally long read range.

Crucially, the reconfiguration is entirely passive-component based, eliminating any need for external power—a decisive advantage over conventional approaches using PIN diodes or MEMS systems that inherently require dedicated power sources.

## 5. CONCLUSION

A frequency-reconfigurable dipole RFID antenna, enhanced with two H-SRR resonators, has been developed to improve adaptability and performance across diverse operational conditions. The inclusion of these resonators allows for better control of electromagnetic behavior, enabling the antenna to adjust its response to varying environments. This innovative design incorporates tunable elements such as variable capacitors, allowing for real-time adjustment of the antenna's resonance frequency. This dynamic tuning capability provides greater flexibility, making the antenna suitable for a wide range of applications. The integration of the Alien Gen2 H4 chip is crucial for extending the antenna's read range, even in scenarios where negative gain values are present. Despite the inherent challenges of operating with reduced gain, the antenna achieves impressive read distances, enhancing its practical application in RFID systems. Special attention has been given to the antenna's performance in metal-rich environments, where traditional RFID systems often struggle. The design has been optimized to mitigate the interference and signal distortion caused by metallic surfaces, enabling efficient operation across multiple UHF frequency bands. Extensive simulations have validated the performance of this reconfigurable antenna. Results indicate that the antenna maintains high performance while adapting to different environmental and operational scenarios. Its ability to dynamically adjust its resonance frequency without compromising efficiency represents a significant advancement in RFID technology. This frequency-reconfigurable RFID antenna offers a new level of flexibility and functionality, making it particularly well-suited for modern RFID applications. Its ability to provide versatile and adaptive communication solutions addresses the growing demand for more responsive and robust RFID systems in industries such as logistics, manufacturing, and asset tracking.

FUNDING INFORMATION

The authors state no funding involved.

AUTHOR CONTRIBUTIONS STATEMENT

This journal uses the Contributor Roles Taxonomy (CRediT) to recognize individual author contributions, reduce authorship disputes, and facilitate collaboration.

Name of Author	C	M	So	Va	Fo	I	R	D	O	E	Vi	Su	P	Fu
Zakaria Errachidi	✓	✓	✓	✓	✓	✓	✓	✓	✓	✓	✓			✓
Jamal Zbitou	✓	✓	✓	✓	✓	✓	✓	✓	✓	✓	✓	✓		
Noha Chahboun	✓				✓					✓	✓	✓		
Otman Oulhaj		✓			✓					✓				
Ahmed Lakhssassi		✓			✓					✓				

C : Conceptualization  
M : Methodology  
So : Software  
Va : Validation  
Fo : Formal analysis  
I : Investigation  
R : Resources  
D : Data Curation  
O : Writing - Original Draft  
E : Writing - Review & Editing  
Vi : Visualization  
Su : Supervision  
P : Project administration  
Fu : Funding acquisition

CONFLICT OF INTEREST STATEMENT

Authors state no conflict of interest.

DATA AVAILABILITY

Data availability is not applicable to this paper as no new data were created or analyzed in this study.

REFERENCES

[1] F. Rahmani, N. A. Touhami, A. B. Kchairi, and N. Taher, "Circular planar antenna with reconfigurable radiation pattern using PIN diodes," *Procedia Manufacturing*, vol. 46, pp. 760–765, 2020, doi: 10.1016/j.promfg.2020.04.001.

[2] S. Souai, "Low-frequency reconfigurable super-directional miniature antenna arrays for IoT (in France: Réseaux d'antennes miniatures super-directifs reconfigurables basses fréquences pour l'IoT)," Ph.D. dissertation, Univ. Tunis El-Manar, Tunis, Tunisia, Apr. 2020.

[3] M. Rammal, "Development of frequency-agile antennas integrating a ferroelectric capacitor (in France: Développement d'antennes agiles en fréquence intégrant un condensateur ferroélectrique)," Ph.D. dissertation, Doctoral School of Science and Engineering for Information and Mathematics, Univ. of Limoges, Limoges, France, 2017.

[4] S. Shrimal, R. Agrawal, I. B. Sharma, and M. M. Sharma, "Dual wideband circularly polarized reconfigurable antenna using gap loaded annular ring," *AEU - International Journal of Electronics and Communications*, vol. 178, p. 155296, 2024, doi: 10.1016/j.aeue.2024.155296.

[5] K. Madhusudhana and S. P. Hegde, "Reconfigurable fractal microstrip antenna with varactor diode," *Global Transitions Proceedings*, vol. 3, no. 1, pp. 183–189, 2022, doi: 10.1016/j.gltp.2022.03.007.

[6] T. M. Benaouf, A. Hamdoun, M. Himdi, O. Lafond, and H. Ammor, "Hybrid coupler used as tunable phase shifter based on varactor diodes," *Micromachines*, vol. 15, no. 7, p. 838, 2024, doi: org/10.3390/mi15070838.

[7] A. Boufrioua, "Frequency reconfigurable antenna designs using PIN diode for wireless communication applications," *Wireless Personal Communications*, vol. 110, no. 4, pp. 1879–1885, 2020, doi: 10.1007/s11277-019-06816-x.

[8] R. J. Chitra and V. Nagarajan, "Frequency reconfigurable antenna using PIN diodes," in *2014 20th National Conference on Communications, NCC 2014*, IEEE, Feb. 2014, pp. 1–4, doi: 10.1109/NCC.2014.6811318.

[9] A. A. Palsokar and S. L. Lahudkar, "Frequency and pattern reconfigurable rectangular patch antenna using single PIN diode," *AEU - International Journal of Electronics and Communications*, vol. 125, p. 153370, 2020, doi: 10.1016/j.aeue.2020.153370.

[10] W. A. Awan, N. Hussain, S. G. Park, and N. Kim, "Intelligent metasurface based antenna with pattern and beam reconfigurability for internet of things applications," *Alexandria Engineering Journal*, vol. 92, pp. 50–62, 2024, doi: 10.1016/j.aej.2024.02.034.

[11] D. Bammedi and C. B. R. Kota, "Design and validation of frequency reconfigurable multiband antenna using varied current distribution method," *Measurement: Sensors*, vol. 29, p. 100844, 2023, doi: 10.1016/j.measen.2023.100844.

[12] D. E. Hadri, A. Zakriti, and A. Zugari, "Reconfigurable antenna for Wi-Fi and 5G applications," *Procedia Manufacturing*, vol. 46, pp. 793–799, 2020, doi: 10.1016/j.promfg.2020.04.007.




[13] ConnectWave, "Normes et standards RFID," *ConnectWave*, 2024. [Online]. Available: <https://www.connectwave.fr/techno-appli-iot/rfid/normes-et-standards/>. (Date accessed: Sep. 01, 2024).

[14] E. Zakaria, Z. Jamal, C. Noha, O. Aziz, and L. Yassin, "Miniaturized UHF RFID tag based on dipole antenna loaded with hexagonal split ring resonators (H-SRR), mounted on metallic objects," in *1st International Conference on Computing, Internet of Things and Microwave Systems, ICCIMS 2024*, IEEE, Jul. 2024, pp. 1–6, doi: 10.1109/ICCIMS61672.2024.10690329.




- [15] R. Marqués, F. Mesa, J. Martel, and F. Medina, "Comparative analysis of edge- and broadside-coupled split ring resonators for metamaterial design - theory and experiments," *IEEE Transactions on Antennas and Propagation*, vol. 51, no. 10 I, pp. 2572–2581, 2003, doi: 10.1109/TAP.2003.817562.
- [16] B. Nasiri, A. Ennajih, A. Errkik, J. Zbitou, and M. Derri, "A novel miniature coplanar band-pass filter for ISM applications," *Bulletin of Electrical Engineering and Informatics*, vol. 9, no. 1, pp. 180–186, 2020, doi: 10.11591/eei.v9i1.1340.
- [17] B. Nasiri, A. Errkik, and J. Zbitou, "A new design of stepped antenna loaded metamaterial for RFID applications," *Bulletin of Electrical Engineering and Informatics*, vol. 10, no. 5, pp. 2661–2666, 2021, doi: 10.11591/eei.v10i5.2675.
- [18] C. Saha and J. Y. Siddiqui, "A comparative analysis for split ring resonators of different geometrical shapes," in *2011 IEEE Applied Electromagnetics Conference, AEMC 2011*, IEEE, Dec. 2011, pp. 1–4, doi: 10.1109/AEMC.2011.6256871.
- [19] C. Saha, J. Y. Siddiqui, D. Guha, and Y. M. M. Antar, "Square split ring resonators: Modelling of resonant frequency and polarizability," in *2007 IEEE Applied Electromagnetics Conference, AEMC 2007*, IEEE, Dec. 2007, pp. 1–3, doi: 10.1109/AEMC.2007.4638039.
- [20] M. Smari, S. Dakhli, J. M. Floc'h, and F. Choubani, "Design of frequency-reconfigurable printed monopole antenna using capacitive loading," in *Mediterranean Microwave Symposium, IEEE*, pp. 1–4, Oct. 2019, doi: 10.1109/MMS48040.2019.9157249.
- [21] S. Dakhli, M. Smari, J. M. Floc'h, and F. Choubani, "Design of frequency-reconfigurable triband dipole antenna using capacitive loading," in *2020 International Wireless Communications and Mobile Computing, IWCMC 2020*, IEEE, pp. 1342–1346, Jun. 2020, doi: 10.1109/IWCMC48107.2020.9148133.
- [22] V. Muzzupapa, L. Huitema, A. Crunteanu, C. Borderon, R. Renoud, and H. Gundel, "Development of ferroelectric variable capacitors and their integration into a frequency-reconfigurable antenna in the millimeter domain (in France: Développement de condensateurs variables ferroélectriques et leur intégration dans une antenne reconfigurable en fréquence dans le domaine millimétrique)," *Ninth Plenary Conference of the GDR ONDES University of Lille*, 2021. (Date accessed: Aug. 17, 2025).
- [23] V. Muzzupapa *et al.*, "Integration of ferroelectric variable capacitors in a frequency reconfigurable antenna in the millimeter domain (in France: Intégration de condensateurs variables ferroélectriques dans une antenne reconfigurable en fréquence dans le domaine millimétrique)," *22nd National Microwave Days*, Limoges, France, 2022.
- [24] I. Rouissi, I. B. Trad, J. M. Floch, H. Rmili, and H. Trabelsi, "Study and design of a frequency reconfigurable square patch antenna for multi-standard telecommunications systems, (in France: Etude et conception d'une Antenne Patch Carré Reconfigurable en fréquence pour les systèmes de télécommunications multistandards)" *19th National Microwave Days*, Bordeaux, France, 2015.
- [25] S. R. Avenue, "RO4000® high frequency circuit materials," pp. 1–4, 2024. [Online]. Available: <https://rogerscorp.com/-/media/project/rogerscorp/documents/advanced-electronics-solutions/english/data-sheets/ro4000-laminates-ro4003c-and-ro4350b--data-sheet.pdf>. (Date accessed: Aug. 15, 2024).
- [26] F. Erman *et al.*, "Low-profile interdigitated UHF RFID tag antenna for metallic objects," *IEEE Access*, vol. 10, pp. 90915–90923, 2022, doi: 10.1109/ACCESS.2022.3201644.
- [27] E. Zakaria, Z. Jamal, L. Mohamed, L. Ahmed, O. Aziz, and C. Noha, "A new design of a spiral UHF RFID tag dipole antenna mounted on metallic objects," in *Mediterranean Microwave Symposium, IEEE*, Oct. 2023, pp. 1–6, doi: 10.1109/MMS59938.2023.10421228.
- [28] A. Technology, "Higgs-4 IC Product Page," *Technology, Alien*, 2022. [Online]. Available: <https://www.alientechnology.com/products/ic/higgs-4/>. (Date accessed: Sep. 01, 2022).
- [29] V. Vitramon, "VJ HIFREQ series - high frequency chip resistors data sheet," *Vishay*, 2024. [Online]. Available: <https://www.vishay.com/docs/45258/vjhifreqseries.pdf>
- [30] K. V. S. Rao, P. V. Nikitin, and S. F. Lam, "Antenna design for UHF RFID tags: A review and a practical application," *IEEE Transactions on Antennas and Propagation*, vol. 53, no. 12, pp. 3870–3876, 2005, doi: 10.1109/TAP.2005.859919.
- [31] P. W. Sarr, I. Dioum, I. Diop, I. Gueye, L. Sane, and K. Diallo, "Frequency reconfigurable UHF RFID dipole tag antenna using a PIN Diode," in *Lecture Notes of the Institute for Computer Sciences, Social-Informatics and Telecommunications Engineering, LNICTST*, pp. 77–86, 2021, doi: 10.1007/978-3-030-90556-9\_7.
- [32] A. Bansal, S. Sharma, and R. Khanna, "RFID tag design with high read range performance for dual band applications in UHF Range," in *2022 IEEE 12th International Conference on RFID Technology and Applications, RFID-TA 2022*, IEEE, Sep. 2022, pp. 82–85, doi: 10.1109/RFID-TA54958.2022.9924081.
- [33] M. Muruges, S. K. A. Rahim, E. H. Lim, and P. S. Chee, "A low-profile patch-loaded ring antenna with wide frequency Tuning capability for dual-band metal-mountable tag design," *IEEE Access*, vol. 12, pp. 176884–176894, 2024, doi: 10.1109/ACCESS.2024.3505217.

## BIOGRAPHIES OF AUTHORS






**Zakaria Errachidi**    was born in Ouezzane, Morocco, in July 1988. He obtained a Bachelor's degree in Physical Sciences and Electronics from Abdelmalek Essaadi University in Tétouan in 2013. In 2015, he earned a Master's degree in Telecommunications from the same university. He is currently pursuing a Ph.D. in Electronics and Telecommunications at Abdelmalek Essaadi University. His research interests include UHF RFID tags and their applications in wireless communications. He can be contacted at email: zakaria.errachidi@etu.uae.ac.ma.






**Pr. Dr. Jamal Zbitou**    was born in Fes, Morocco, in June 1976. He received the Ph.D. degree in electronics from Polytech of Nantes, the University of Nantes, France, in 2005. He is currently Full Professor of Electronics in ENSA of Tetuan, Abdelmalek Essaadi University Morocco. He is involved in the design of hybrid, monolithic active and passive microwave electronic circuits. He is involved also in the design of rectennas, RFID tag and their applications in wireless communications, and wireless power transmission (WPT). He is the General Chair of the International Conference on Computing and Wireless Communication Systems ([www.iccwcs.net](http://www.iccwcs.net)). He is the author/co-author of more than 205 scientific Scopus Indexed publications and Editor of Four Handbooks and Book, and thesis advisor and Co-advisor of 35 Ph.D. Students. He can be contacted at email: [j.zbitou@uae.ac.ma](mailto:j.zbitou@uae.ac.ma).






**Noha Chahboun**    was born in Chefchaouen, (Morocco) in 1969. She obtained her doctorate in 1994 at Cadi Ayyad University in Marrakech (Morocco) where she worked on ternary semiconductors thin films for optoelectronic devices. She has been an assistant professor since September 1995; first at the Faculty of Sciences of Marrakech and from July 1999 at the National School of Applied Sciences of Tangier (Morocco) - Abdelmalek Essaadi University. Her research is currently focused on the design of antennas based on metamaterials and metasurfaces particularly for 5G mobile communications. She can be contacted at email: [n.chahboun@uae.ac.ma](mailto:n.chahboun@uae.ac.ma).



**Otman Oulhaj**    was born in Tetuan, Morocco, in 1981. He received the B.C. of Science in Electronic from Abdelmalek Essaadi University, Tetuan, Morocco, in 2004. He received the master's degree in Electronic and Telecommunication from Abdelmalek Essaadi University, Tetuan, Morocco, in 2012. He is currently an associate Professor of Electronics and telecommunication Abdelmalek Essaadi University, FP of Larache, Morocco, He is involved in the design of microwave electronic circuits. He can be contacted at email: [o.oulhaj@uae.ac.ma](mailto:o.oulhaj@uae.ac.ma).



**Ahmed Lakhssassi**    responsible of the LIMA laboratory CANADA, received the B.Ing. and M.Sc. in electrical engineering from Université du Québec (UQTR), Québec, Canada in 1988 and 1990 respectively. He also received the Ph.D. in Energy and Material sciences in 1995 from INRS-Energie et Matériaux Montréal, Québec, Canada. A year also, he had become a professor of Electro-thermo-mechanical aspects at NSERC -Hydro-Quebec Industrial Research Chair at Electrical Engineering Department of the UQTR. Since 1998, he has been with UQO (Université du Québec en Outaouais), where he is currently titular professor and responsible of the LIMA laboratory LIMA (Advanced Microsystem Engineering Laboratory) developing algorithms for Microsystems thermo-mechanical monitoring and associated distributed sensors network. His research interest is the fields of automatic IP porting tools between different technology nodes and LAIC systems thermo-mechanical prediction unit and monitoring methods to sustain transient thermomechanical stress peaks reliability. He is the author/co-author of more than 150 scientific publications and research report, and thesis advisor of 60 graduate and undergraduate students who completed their studies. He can be contacted at email: [ahmedlakhssassi@gmail.com](mailto:ahmedlakhssassi@gmail.com)